Dynamics of heterogeneous hard spheres in a file

Ophir Flomenbom
Flomenbom-BPS, 19 Louis Marshal Street, Tel Aviv 62668, Israel

(Received 17 May 2010; revised manuscript received 13 July 2010; published 21 September 2010)

Normal dynamics in a quasi-one-dimensional channel of length L ($\rightarrow\infty$) of N hard spheres are analyzed. The spheres are heterogeneous: each has a diffusion coefficient D that is drawn from a probability density function (PDF), $W \sim D^{-\gamma}$ for small D, where $0 \leq \gamma < 1$. The initial spheres' density ρ is nonuniform and scales with the distance (from the origin) l as $\rho \sim l^{-\alpha}$, $0 \leq \alpha \leq 1$. An approximation for the N-particle PDF for this problem is derived. From this solution, scaling law analysis and numerical simulations, we show here that the mean square displacement for a particle in such a system obeys $\langle r^2 \rangle \sim t^{(1-\gamma)/(2c-\gamma)}$, where $c = 1/(1+\alpha)$. The PDF of the tagged particle is Gaussian in position. Generalizations of these results are considered.

DOI: 10.1103/PhysRevE.82.031126 PACS number(s): 05.40.−a, 66.30.Pa, 87.10.−e

I. INTRODUCTION

Diffusion is among the fundamental processes in condensed-matter physics, chemistry, and biology, as it affects the behavior of many complex processes in these fields (e.g., [1–4]). An important process in the study of diffusion is file dynamics (also known as single file dynamics) [4–37,40]. Put simply, it is a process of N identical particles (hard spheres) that perform normal stochastic diffusion, with the same diffusion coefficient D, in a cylinder or a strait, of length L ($L \rightarrow \infty$). The mean particles' density, ρ, is fixed: $\rho = \rho_0 = N/L$. (This means that the mean microscopic distance between adjacent hard spheres is fixed and follows $\Delta = L/N$, where Δ cannot be smaller than the particle's diameter.) The dynamics of hard spheres in a strait is a very realistic model for many microscopic processes [1,30–37]: for example, (a) diffusion within biological and synthetic pores and in porous materials of water, ions, proteins, and organic molecules [1,30]; (b) diffusion along one-dimensional objects, such as the motion of motor proteins along filaments [1]; (c) conductance of electrons in nanowires [37]; and (d) single file dynamics has also been related to monomer dynamics in a polymer: both systems share a similar scaling law for the mean square displacement (MSD) of a tagged monomer [29,34].

The most well-know property of file dynamics is the scaling of the MSD $\langle r^2 \rangle$ of a tagged particle in the file: $\langle r^2 \rangle \approx (Dt)^{1/2}/\rho_0$. This result is unique. It is much slower than the MSD of a free mesoscopic particle diffusing in solution, for which $\langle r^2 \rangle_{free} \approx Dt$. Clearly, a tagged particle in a file is much slower than a free particle as it can only move when other particles move in the same direction. Still, the special scaling of $\langle r^2 \rangle$ with time reflects a unique mechanism of motion. In Ref. [23], we have derived a general relation connecting the mean absolute displacement (MAD) of a free particle and of a tagged particle in a file (that have the same underlying dynamics) that captures some of this uniqueness,

$$\langle |r| \rangle \approx \langle |r| \rangle_{free}/n. \tag{1}$$

Here, n is the number of particles in the covered length $\langle |r| \rangle$. Equation (1) holds when the file has a fixed density on average ($\langle |r| \rangle \approx n/\rho_0$), and this leads to

$$\langle |r| \rangle \approx \rho_0^{-1/2} \langle |r| \rangle_{free}^{1/2}. \tag{2}$$

Equations (1) and (2) show that when diffusing a distance r, the tagged particle slows down relative to a free particle as it can only move when coordination with the file particles is achieved, and this coordination is proportional to 1 over the number of particles in the distance r. The relation in Eq. (2) leads to the famous MSD in a Brownian file, that is, $\langle r^2 \rangle \approx (Dt)^{1/2}/\rho_0$.

Yet, there are many other known statistical properties of file dynamics [4–27]. (a) The probability density function (PDF) of the tagged particle is asymptotically a Gaussian in position [5]. (b) The motion of the particles is correlative; namely, a cloudlike motion is seen in the system [9,18]. This cloud of particles is not of a constant density; namely, fluctuations in the particles' density are observed [9,18]. (c) The microscopic single event PDFs in time and space have finite moments [17]. (d) In dimensions larger than 1, a tagged hard sphere in the presence of hard spheres diffuses normally [9]; namely, in such a system the MSD of a tagged particle is linear with time. (e) For a deterministic basic single file with momentum exchange upon collisions, the tagged particle's PDF is also a Gaussian, yet with a variance that scales as the time [6] [note that Eq. (2) still holds]. (f) We note that in this paper, the statistics of the particles at the edges of the file are not considered as special particles. Indeed, in a file with a finite number of particles, yet of infinite length (namely, $l \rightarrow \infty$), the particles at the edge of the file can diffuse freely to the side not bounded by particles. For an analysis that focuses on this point, see Ref. [25]. Here, we focus on files with $N \rightarrow \infty$, where the tagged particle represents the particles in the middle of the file.

Still, in realistic systems, one or several of the conditions defining the *basic* file may break down, and this may lead to different dynamical behaviors. For example, in a real channel, the particles may bypass each other with a constant probability upon collisions [19–22], and this leads to an enhanced diffusion. Yet, when the particles interact with the channel, a slower diffusion is seen [15]. An important generalization in file dynamics takes the initial particles' density law to scale with the distance l [23],

$$\rho(l) = \rho_0 (l/\Delta)^{-\alpha}, \quad 0 \leq \alpha \leq 1. \tag{3}$$

$\rho(l)$ in Eq. (3) is the initial density of the file: the particles are initially positioned at $x_{0,j} = \mathrm{sgn}(j)\Delta |j|^{1/(1-\alpha)}$ for $|j|$

$\leq M$, $N=2M+1$. So, the initial number of particles n as a function of the length l obeys $n=(l/\Delta)^{1-\alpha}$. Among the possible realistic choices for a particle distance law (e.g., an exponential, a Gaussian, or a power law) the one that affects the dynamics is a power law. This is shown when calculating the MAD for a system obeying Eq. (3) [23],

$$\langle|r|\rangle \approx \rho_0^{(\alpha-1)/2}\langle|r|\rangle_{free}^{(1+\alpha)/2}. \tag{4}$$

When $\alpha\to 0$, we recover the standard result $\langle|r|\rangle \approx \rho_0^{-1/2}\langle|r|\rangle_{free}^{1/2}$. This equation means that only a power-law density law can influence the dynamics; namely, when the distance between particles along the file does not increase fast enough, as in a power-law density law, the scaling of the MAD is not affected by the fluctuations in the distance among particles.

Now, $\langle|r|\rangle$ in Eq. (4) holds for *any* renewal N-body underlying dynamics and for the density in Eq. (3). Here, a renewal file is a file in which all the particles attempt jumping at the same time. We use the term of renewal process in accordance of this term in probability theory [39].

Equation (4) generalizes Eq. (2). Still, this generalization is limited to the other conditions of a basic file. In this paper, we deal with heterogeneous files. In a heterogeneous file, the particles' diffusion coefficients are distributed according to a PDF; here, we use

$$W(D) = \frac{1-\gamma}{\Lambda}\left(\frac{D}{\Lambda}\right)^{-\gamma}, \quad 0 \leq \gamma < 1, \tag{5}$$

where Λ is the fastest possible diffusion coefficient in the file. The initial conditions are distributed according to Eq. (3). In a series of analytical and numerical calculations, we show here that the MSD for the tagged particle in such a file follows:

$$\rho_0^2\langle r^2\rangle \sim (\rho_0^2\Lambda t)^{(1-\gamma)/(2c-\gamma)}, \quad c = 1/(1+\alpha). \tag{6}$$

The corresponding PDF is a Gaussian. Generalizations and implications of these results are considered.

II. CALCULATING THE FILE'S PDFS

In this paragraph we calculate the PDF of the tagged particle in a heterogeneous file from the joint PDF for all the particles in the file, $P(\boldsymbol{x},t|\boldsymbol{x_0})$. Here, $\boldsymbol{x} =\{x_{-M},x_{-M+1},\ldots,x_M\}$ is the set of particles' positions at time, t, and $\boldsymbol{x_0}$ is the set of the particles' initial positions at the initial time, t_0, which is set to zero. The tagged particle is taken as the middle particle in the file. The following calculations for $P(\boldsymbol{x},t|\boldsymbol{x_0})$ are based on our analysis of simple files [23], and so we concisely present these calculations first; the curious reader can also find an elaborated discussion of our previous calculations in Appendix A of the supplementary material in this paper [42].

Simple files. In a simple file, $P(\boldsymbol{x},t|\boldsymbol{x_0})$ obeys a simple normal diffusion equation,

$$\partial_t P(\boldsymbol{x},t|\boldsymbol{x_0}) = D\sum_{j=-M}^{M}\partial_{x_j}\partial_{x_j}P(\boldsymbol{x},t|\boldsymbol{x}_0). \tag{7}$$

Equation (7) is solved with the appropriate boundary conditions, which reflect the hard-sphere nature of the system:

$$[D\partial_{x_j}P(\boldsymbol{x},t|\boldsymbol{x}_0)]_{x_j=x_{j+1}} = [D\partial_{x_{j+1}}P(\boldsymbol{x},t|\boldsymbol{x}_0)]_{x_{j+1}=x_j}$$

for

$$j=-M,\ldots,M-1$$

and with the appropriate initial condition

$$P(\boldsymbol{x},t\to 0|\boldsymbol{x}_0) = \prod_{j=-M}^{M}\delta(x_j-x_{0,j}). \tag{8}$$

The PDFs' coordinates must obey the order $x_{-M}\leq x_{-M+1} \leq\cdots\leq x_M$. The solution of Eq. (7) is a sum of products of Gaussians [23–27],

$$P(\boldsymbol{x},t|\boldsymbol{x}_0) = \frac{1}{c_N}\sum_p \exp\left(\frac{-1}{4Dt}\sum_{j=-M}^{M}[x_j-x_{0,j}(p)]^2\right). \tag{9}$$

In Eq. (9), the external sum is over $N!$ permutations of the initial conditions. The factor that takes care for the normalization is c_N; c_N is always the normalization constant everywhere it appears in this paper. Equation (9) is understood under the condition that the coordinates are ordered. Equation (9) is a direct result of the Bethe ansatz for linearly coupled particles [38].

Equation (9) is the starting point for finding the PDF of a tagged particle in this file, $P(r,t|r_0)$. In Ref. [23], we have estimated this PDF as

$$P(r,t|r_0) \approx \frac{1}{c_N}\sum_{\tilde{p}}\exp\left(\frac{-1}{4Dt}\sum_{j=-n}^{n}[r_d-x_{0,j}(\tilde{p})]^2\right)$$
$$\leq \frac{1}{c_N}\exp\left(\frac{-r_d^2}{2Dt}\sum_{j=1}^{n}1\right). \tag{10}$$

In Eq. (10), $r_d=r-r_0$. Equation (10) is a result of lengthy calculations and assumes the limit of long times. The full details of the calculations that relate Eqs. (9) and (10) were presented in Ref. [23]; yet, these are presented in Appendix A of the supplementary material in this paper [42]. In what follows, we highlight the important steps of these calculations. We start with Eq. (9) and first integrate the file coordinates excluding the tagged particle's coordinate. Then, we count the important permutations that contribute to the sum of permutations after the integration; then, these form the values of $\tilde{p}$. Once we know the set $\{\tilde{p}\}$, we can further estimate $P(r,t|r_0)$ with the inequality. The inequality simplifies the expression for $P(r,t|r_0)$ as the last term in Eq. (10) is a summation over a constant; namely, the sum counts particles, and so its solution is n: the number of particles in the length $\tilde{r}$. $\tilde{r}$ is found from the equation

$$\frac{\tilde{r}(n)}{\sqrt{4Dt}} = 1.$$

This relation for $\tilde{r}$ is a result of our approximation that each exponential factor is a kind of a step function where the step function is nonzero for a width equal to the variance of the exponential argument. As in a constant density file the distance is proportional to the number of particles in it, $n \sim\tilde{r}/\Delta$; we have $n\sim\sqrt{Dt}/\Delta$ and, thus,

$$P(r,t|r_0) \leq \frac{1}{c_N} e^{(-r_d^2/2Dt)n} = \frac{1}{c_N} e^{-R_d^2/\sqrt{2\tau}},$$

where $R_d = r_d/\Delta$ and $\tau = \Delta^{-2}Dt$ are the dimensionless distance and time, respectively.

Heterogeneous files. Once the relation connecting Eqs. (9) and (10) is established, we can use a corresponding relation for deriving the PDF of the tagged particle in a heterogeneous file. Clearly, we need first to solve the equation of motion for the N-particle PDF for this file,

$$\partial_t P(\boldsymbol{x},t|\boldsymbol{x_0}) = \sum_{j=-M}^{M} D_j \partial_{x_j} \partial_{x_j} P(\boldsymbol{x},t|\boldsymbol{x}_0), \tag{11}$$

subjected to the boundary conditions

$$[D_j \partial_{x_j} P(\boldsymbol{x},t|\boldsymbol{x_0})]_{x_j = x_{j+1}} = [D_{j+1} \partial_{x_{j+1}} P(\boldsymbol{x},t|\boldsymbol{x_0})]_{x_{j+1}=x_j},$$

$$j = -M, \ldots, M-1 \tag{12}$$

and with the initial condition [Eq. (8)]. We *approximate* the solution of Eqs. (11) and (12) with

$$P(\boldsymbol{x},t|\boldsymbol{x_0}) \approx \frac{1}{c_N} \sum_p \exp\left(- \sum_{j=-M}^{M} \frac{[x_j - x_{0,j}(p)]^2}{4tD_j} \right). \tag{13}$$

Equation (13) is our first main result in this paper. This equation was written in analogy with Eq. (10). To test the quality of the approximation, we plug it in the diffusion equation for a heterogeneous file [Eq. (11)]. We find that Eq. (13) indeed fulfills Eq. (11). Equation (13) also fulfills the initial condition [Eq. (8)]. Yet, Eq. (13) only approximates the boundary conditions [Eq. (12)]. Nevertheless, a simple analysis shows that the approximation in Eq. (13) becomes more and more accurate for large times. (A full analysis of Eq. (13) is presented in Appendix B of the supplementary material in this paper [42].)

Using Eq. (13), we approximate the PDF of the tagged particle in the heterogeneous file with

$$P(r,t|r_0) \approx \frac{1}{c_N} \sum_{\tilde{p}} \exp\left(- \sum_{j=-n}^{M} \frac{[r_d - x_{0,j}(\tilde{p})]^2}{4tD_j} \right)$$

$$\leq \frac{1}{c_N} \exp\left(\frac{-R_d^2}{4\tau} \sum_{j=1}^{n} 1/D_j \right). \tag{14}$$

Here, $\tau = \Delta^{-2}\Lambda t$. Equation (14) is based on the same approach that relates Eq. (9) to Eq. (10). (Additional technical comments on this relation are presented in Appendix C of the supplementary material in this paper [42].) Yet for proceeding, we need to calculate the sum in last factor in Eq. (14). These calculations are more complicated than those performed for the simple file. First, for a heterogeneous file that its diffusion coefficients are drawn from Eq. (5), any group of n particles (taken from the N particles in the file) must have the following values for their diffusion coefficients:

$$D_j \approx \Lambda[1 - (j-1)/n]^{1/1-\gamma}, \quad 1 \leq j \leq n,$$

where the values of the diffusion coefficients are ordered from the largest to the smallest. This relation's accuracy increases as $n \to \infty$. (For its derivation, see Appendix D of the supplementary material in this paper [42].) Second, we need to find $n(t)$. This is found from the equation

$$\frac{\tilde{r}(n)^2}{\tilde{D}_n} = t. \tag{15}$$

Equation (15) represents the arguments in all the exponentials in Eq. (14). $\tilde{r}(n)$ is simply found from the density law in the system, $n \approx (\tilde{r}/\Delta)^{1-\alpha}$. The diffusion coefficient $\tilde{D}_n$ appearing in Eq. (15) must represent a bunch of slow particles in the interval that has in it n particles, as these particles affect the result the most. Yet, $\tilde{D}_n$ is a typical slow-diffusion coefficient and not necessarily the slowest. We estimate $\tilde{D}_n$ with $\tilde{D}_n = \Lambda n^{-\gamma/(1-\gamma)}$. The derivation of this relation is spelled out in the next paragraph (Sec. III). Here, we note that as γ tends to 1, $\tilde{D}_n$ reaches the value of the slowest diffusion coefficient from a group of n particles. Yet, for a relative fast system $\tilde{D}_n$ approaches a constant independent of n. A similar trend is seen in the behavior of the average diffusion coefficient, which vanishes as γ goes to 1 and has a nonzero value as γ tends to 0. Now, using the above expressions for $\tilde{r}(n)$ and $\tilde{D}_n$ in Eq. (15), we find

$$n \approx \tau^{(1-\alpha)(1-\gamma)/(2-\gamma)(1+\alpha)}. \tag{16}$$

Substituting Eq. (16) in Eq. (14) yields the PDF for the tagged particle in a heterogeneous file,

$$P(r,t|r_0) \leq \frac{1}{c_N} \exp\left[\frac{-R_d^2}{4\tau} \sum_{j=1}^{n} \left(1 - \frac{j-1}{n} \right)^{-1/(1-\gamma)} \right]$$

$$= \frac{1}{c_N} \exp\left(\frac{-R_d^2}{4\tau} n^{1/(1-\gamma)} \right)$$

$$= \frac{1}{c_N} \exp\left(\frac{-R_d^2}{4\tau} \tau^{(1-\alpha)/[2-\gamma(1+\alpha)]} \right). \tag{17}$$

A Gaussian PDF is specified through its variance and so,

$$\langle R_d^2 \rangle = 2\tau^{(1-\gamma)/(2c-\gamma)}, \quad c = 1/(1+\alpha). \tag{18}$$

Equations (17) and (18), together with Eq. (13), are the major results in this paper. Note that Eq. (18) is obtained from Eq. (17), and so it is the upper bound of the MSD of this file. Yet, we show in what follows, in scaling law analysis and in simulations, that this is, in fact, the asymptotic limit of the actual MSD.

Examining Eq. (18), we note the following. In the limit of $\gamma \to 0$, $\langle R_d^2 \rangle \sim \tau^{(1+\alpha)/2}$. This result is equivalent to Eq. (4) for a Brownian file. This result means that when there are not enough slow particles in the file, the MSD scales in the same way as of a simple file. Thus, this result gives the criteria when $W(D)$ affects the diffusion process significantly. In the limit of a constant density, $\alpha = 0$, we have $\langle R_d^2 \rangle \approx \tau^{(1-\gamma)/(2-\gamma)}$. Here, when $\gamma \to 1$, $\langle R_d^2 \rangle \approx 1$, namely, in this limit the system is frozen. Equation (18) also predicts a cancellation of opposing effects: slow diffusion due to many slow particles and fast diffusion due to a low particles' density can cancel each other; when $\alpha=\gamma/(2-\gamma)$, a simple file scaling is seen $\langle R_d^2\rangle \sim \tau^{1/2}$, yet the actual file is heterogeneous.

Finally, we note here that a very different result for the MSD than Eq. (18) is obtained in a heterogeneous file obeying Eq. (5) when all the particles start at the origin (see Ref. [25] for a discussion).

III. SCALING LAW ANALYSIS

In this paragraph, we derive a scaling law for $\langle|r|\rangle$ in a heterogeneous file with a constant density. The results of this paragraph support Eq. (18) and further illuminate heterogeneous files. We start with the following set of relations:

$$\langle|r|\rangle=\langle|r|\rangle_{free}/n=\Delta^{1/2}\langle|r|\rangle_{free}^{1/2}\approx\Delta^{1/2}[D(\langle|r|\rangle_{free})t]^{1/4}. \tag{19}$$

Equation (19) is similar to Eq. (1): n is the number of particles in the cover length, yet $\langle|r|\rangle_{free}$ reflects a free particle dynamics with a *modified diffusion coefficient*, $\langle|r|\rangle_{free}\approx[D(\langle|r|\rangle_{free})t]^{1/2}$. $D(\langle|r|\rangle_{free})$ should reflect the fact that in an interval of length $\langle|r|\rangle_{free}$ there is a typical diffusion coefficient that represents all the particles in this length, as we substitute one for many. Clearly, $D(\langle|r|\rangle_{free})$ is among the slowest ones in the interval $\langle|r|\rangle_{free}$. Still, it should represent a bunch of slow particles and not merely the slowest one. For estimating $D(\langle|r|\rangle_{free})$, we first derive the PDF of the smallest diffusion constant, D_{min}, among n particles, denoted with $f(D_{min},n)$. The diffusion coefficients of the particles are drawn independently of each other, and so this PDF obeys

$$f(D_{min},n+1)=W(D_{min})\left(\int_{D_{min}}^{\Lambda}W(D)dD\right)^n. \tag{20}$$

The factor $W(D_{min})$ represents the PDF that the slowest diffusion coefficient has a value of D_{min} and the integral to the power of n is the probability that all the other particles have diffusion coefficients that are larger than D_{min}. A normalization constant does not affect the following calculations, and it is omitted. Using Eq. (5) in Eq. (20), we find (for $n\gg 1$)

$$f(D_{min},n+1)\approx(D_{min}/\Lambda)^{-\gamma}e^{-n(D_{min}/\Lambda)^{1-\gamma}}. \tag{21}$$

Equation (21) has the typical form of a PDF in extreme value statistics [38]. We use this PDF to link a typical small diffusion coefficient to n. For this, we look on the exponential factor in the PDF, $e^{-n(D_{min}/\Lambda)^{1-\gamma}}$, and notice that only when the condition $n(\tilde{D}_{min}/\Lambda)^{1-\gamma}=1$ is met, a large probability can be assigned for small values of D_{min}. Solving for $\tilde{D}_{min}$, we find $\tilde{D}_{min}=\Lambda n^{-1(1-\gamma)}$. Using $\tilde{D}_{min}$ in Eq. (21) leads to

$$f(\tilde{D}_{min},n)\approx\Lambda^{-1}n^{\gamma/(1-\gamma)}. \tag{22}$$

We define the typical value for the slowest particles in the interval of n particles ($n\gg 1$), denoted as $\tilde{D}_n$, as one over the PDF $f(\tilde{D}_{min},n)$,

$$\tilde{D}_n\equiv 1/f(\tilde{D}_{min},n)\approx\Lambda n^{-\gamma/(1-\gamma)}. \tag{23}$$

Equation (23) was used in the previous paragraph to derive Eq. (17). Substituting Eq. (23) into Eq. (19), with $D(\langle|r|\rangle_{free})\to\tilde{D}_n$ and n in Eq. (16), leads to

$$\langle|R_d|\rangle=\tau^{(1-\gamma)/2(2-\gamma)}. \tag{24}$$

Equation (24) is the same as Eq. (18) for $\alpha=0$, with $\langle R_d^2\rangle\approx\langle|R_d|\rangle^2$. Namely, Eq. (24) supports the results obtained in the previous paragraph. Indeed, both calculations rely on the same form for $\tilde{D}_n$, yet these calculations have different starting points. Note that the scaling law considered here holds for $\alpha=0$. In a file with a nonuniform particles' density, the file's density does not scale with the distance in the sense that a given interval of length l taken from the file at different locations along the file has a different density of particles. Thus, any scaling law for a nonfixed density file must rely significantly on known results. Starting from Eq. (19), we do not need to rely on known results. Yet, the reader can find in Ref. [23] a scaling law analysis that uses also known results in deriving scaling laws for nonuniform files.

Scaling law analysis enables to generalize the results for files with different kinds of dynamics. We consider in what follows heterogeneous-deterministic files. A deterministic file is a file in which the particles are Newtonian and each particle is assigned an initial velocity $\pm v$ with equal probability. In a simple deterministic file, the PDF of a tagged particle is a Gaussian with a variance that scales linearly with time. What is $\langle|R_d|\rangle$ when the value $|v|$ is drawn from a PDF of the form of Eq. (5) with equal probability for any direction? Starting from Eq. (19), we find

$$\langle|R_d|\rangle=(\Delta^{-1}|\tilde{v}|t)^{(1-\gamma)/(2-\gamma)}, \tag{25}$$

where $|\tilde{v}|$ is a characteristic velocity in the system. Equation (25) is calculated in a similar way to the analysis of this paragraph. Equation (25) shows that as $\gamma\to 1$ the deterministic file freezes and as $\gamma\to 0$ the file behaves as a simple deterministic file.

IV. NUMERICAL SIMULATIONS

We perform *off*-lattice simulations of Eq. (11) with hardcore interactions between point particles. The fact that the particles are pointlike reflects the equation of motion, yet, does not change the long-time statistics of the file compared to simulations of files on lattices. (In fact, simulations are always latticelike as the smallest length scale is limited by the precision of the machine.) In the simulations, each particle is assigned a diffusion coefficient from the PDF in Eq. (5) ($\Lambda=1$ in the simulation). The jth particle is positioned at $x_{0,j}=\mathrm{sgn}(j)|j|^{1/(1-\alpha)}\Delta$ ($\Delta=1.3$ in the simulation). We set $N=501$ particles. In each time step ($dt=0.13$ in the simulations), each particle is moved relative to its position according to the equation $dx_j=2(q-1/2)\sqrt{2D_jt}$, where q is a random number from the unit PDF and is chosen for each particle at each time step. The particles' locations are ordered after each time step. The interval's length is bound: edge particles cannot move further than their initial conditions

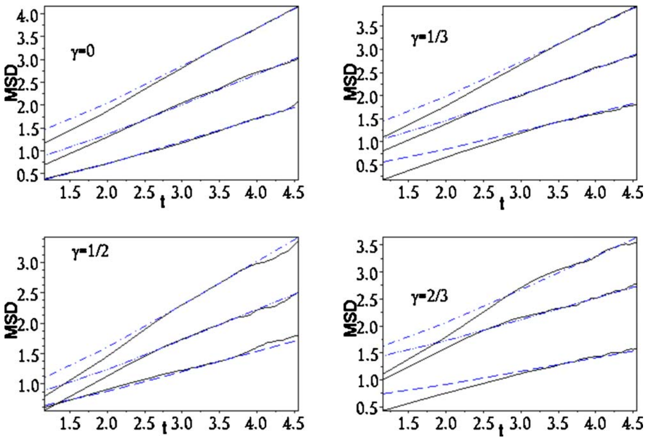

FIG. 1. (Color online) The mean square displacement (MSD) on a log-log scale from 12 different simulations. Each simulation has a specific value for α and γ, where $\gamma=0,1/3,1/2,2/3$ and $\alpha=0,1/3,2/3$. Each panel has a constant value of γ (the smallest value of γ is in the top right panel and γ increases in a z-like shape). Each curve (in a given panel) corresponds to a different value of α, where a lower curve always has a smaller value of α. The analytical curves from Eq. (18) are also shown and coincide nicely with the results from the simulations. [The free parameter of any analytical curve is always chosen to coincide best with the curve of the simulation. Yet, the curve's slope is obtained from Eq. (18).] Note that the x axis in the figure was obtained when monitoring the value of t_j every 10^{Aj} time units (A is a number) and then taking the logarithm of the time vector. The Y axis is the logarithm of the monitored MSD.

plus a room for several full jumps in the direction that extends the initial interval length. The above iteration scheme is executed over and over and over again (three million time steps are used in each simulation). Note that in the above simulations' rules, the boundary conditions are *always* fulfilled. Also, note that the above simulations' rules were also used for simple files, e.g., files with the same diffusion coefficient. Yet, these rules hold also for the heterogeneous file. Here, the reflection principle (that is, the ordering of the particles after each cycle of jumps) represents (a) elastic collisions among particles that can clearly also represent particles with distribution of diffusion coefficients and (b) Brownian dynamics, so the particles momenta decay after each jump relatively fast, and so in the next cycle of jumps the particles do not drag previous velocities.

We perform extensive simulations. Each simulation has different values for α and γ where $\alpha=0,1/3,2/3$ and $\gamma=0,1/3,1/2,2/3$. In each simulation, we calculate the MSD for 30 particles from the file. For each simulation (defined with a specific values for γ and α), the run time for the simulation and the MSD calculations is 3 min on a standard 3.37 GHz PC.

Figure 1 presents the results for the MSD from all the simulations. Each panel shows MSD curves for three values of α each with the same value of γ. The analytical curves obtained from Eq. (18) are also shown. The curves coincide with the numerical results to a satisfactory level. The only point to note is that as α increases, converges occur at larger times. This is an expected behavior for a file with nonfixed particle's density.

In light of the simulations' results, a final remark is made on the interpretation of the limit of long times. In this paper, we used this limit in deriving the statistics of the file. We gave along the paper and in the Appendixes several interpretations for this limit. Yet, we can use Fig. 1 for further defining the meaning of long times. Figure 1 shows that this limit depends on the value of γ and α: when γ and/or α are large, the coincidence of the simulations' curves and the curves obtained from Eq. (18) happens at relatively larger times; plus, at smaller times, the difference among the curves is, in most cases, larger when γ and α are larger. So, we say that long time corresponds to the time, t^*, it takes a particle to reach a distance r^* from its origin that has n^* particles in it. t^* is then estimated with Eq. (18): $r^* \sim \Delta n^{*1/(1-\alpha)} \sim \Delta\sqrt{\langle R_d^2\rangle}$. These relations give $t^* \sim (\Delta^2/\Lambda) n^{*2/[\mu(1-\alpha)]}$, where μ is the scaling power in Eq. (18). We use $n^*=35$ as a safe bound for t^*, as the value of 35 (events) is considered a large number in statistics. From Fig. 1, it is clear that also for $n^* \approx 9$ the coincidence among the simulations' results and the curves obtained from Eq. (18) is excellent.

V. CONCLUDING REMARKS

This paper deals with normal stochastic dynamics of heterogeneous hard spheres in a very long strait. Each sphere has a random diffusion coefficient drawn from a PDF, $W(D) \sim D^{-\gamma}$, $0 \le \gamma < 1$, for small D. The initial positions are also distributed such that the initial particles' density law obeys $\rho(l) \sim \rho_0 (l/\Delta)^{-\alpha}$, $0 \le \alpha \le 1$, where l is the distance from the origin. We first derive the approximation for the particles' PDF for heterogeneous files:

$$P(\boldsymbol{x},t|\boldsymbol{x_0}) \approx \frac{1}{c_N} \sum_p \exp\left(\frac{-1}{4t} \sum_{j=-M}^{M} \frac{[x_j - x_{0,j}(p)]^2}{D_j}\right).$$

From this PDF, we derive the statistics of the tagged particle in heterogeneous files:

$$P(r,t|r_0) \sim \frac{1}{c_N} e^{-R_d^2/2\langle R_d^2\rangle},$$

and

$$\langle R_d^2\rangle = 2\tau^{(1-\gamma)/(2c-\gamma)}, \quad c = 1/(1+\alpha).$$

The same results for the tagged particle's MSD were obtained using additional two approaches: scaling law analysis and numerical simulations. We also obtained results for deterministic files with a constant particles' density and distribution in velocities of the form of Eq. (5); here, using scaling law analysis, we found that the MAD obeys $\langle |R_d| \rangle \sim \tau^{(1-\gamma)/(2-\gamma)}$. All the above results are useful for files in which the particles are not identical and differ in, for example, mass, size, or composition.

Still, there is an interesting generalization of the above; this deals with anomalous files. In an anomalous file, the underlying dynamics are such that the waiting time PDF for individual jumps decays like a power law. (A waiting time PDF in a Brownian file decays exponentially.) Anomalous files may exhibit a rich spectrum of behaviors. We find in preliminary calculations that the nature of the anomaly of the file determines its statistical behaviors. For example, renewal-anomalous files, in which all the particles attempt jumping at the same time, are different than nonrenewal-anomalous files, where each particle has its own clock of waiting times [28]. Also, anomalous files with fluctuating diffusion coefficients may lead to interesting phenomena; this statement relied on a corresponding system with a free particle: when a free stochastic particle performs anomalous dynamics and its diffusion coefficient is drawn every jump from a distribution, a transition in the rule for the power that governs the effective waiting-time PDF of the dynamics is seen [41]. Further analysis of anomalous files is still to come.

ACKNOWLEDGMENT

Funding for this work partially came from The Ministry of Immigrant Absorption of the State of Israel, The Center for Absorption in Science.

[1] B. Alberts, D. Bray, J. Lewis, M. Raff, K. Roberts, and J. D. Watson, *Molecular Biology of the Cell* (Garland Publishing, Inc., London, NY, 1994).
[2] N. G. van Kampen, *Stochastic Processes in Physics and Chemistry* (revised and enlarged edition) (North-Holland, Amsterdam, 1992).
[3] G. H. Weiss, *Aspects and Applications of the Random Walk* (North-Holland, Amsterdam, 1994).
[4] T. M. Liggett, *Interacting Particle Systems* (Springer, New York, 1985).
[5] T. E. Harris, J. Appl. Probab. **2**, 323 (1965).
[6] D. W. Jepsen, J. Math. Phys. **6**, 405 (1965); J. L. Lebowitz and J. K. Percus, Phys. Rev. **155**, 122 (1967).
[7] D. G. Levitt, Phys. Rev. A **8**, 3050 (1973).
[8] C. Rödenbeck, J. Kärger, and K. Hahn, Phys. Rev. E **57**, 4382 (1998).
[9] H. van Beijeren *et al.*, Phys. Rev. B **28**, 5711 (1983).
[10] M. Kollmann, Phys. Rev. Lett. **90**, 180602 (2003).
[11] M. D. Jara and C. Landim, Ann. Inst. Henri Poincare, Sect. A **42**, 567 (2006).
[12] P. Kalinay and J. K. Percus, Phys. Rev. E **76**, 041111 (2007).
[13] K. Hahn and J. Kärger, J. Phys. A **28**, 3061 (1995).
[14] K. Hahn and J. Kärger, J. Chem. Phys. **100**, 316 (1996).
[15] A. Taloni and F. Marchesoni, Phys. Rev. Lett. **96**, 020601 (2006).
[16] D. S. Sholl and K. A. Fichthorn, Phys. Rev. E **55**, 7753 (1997).
[17] F. Marchesoni and A. Taloni, Phys. Rev. Lett. **97**, 106101 (2006).
[18] S. Alexander and P. Pincus, Phys. Rev. B **18**, 2011 (1978).
[19] R. Kutner, H. Van Beijeren, and K. W. Kehr, Phys. Rev. B **30**, 4382 (1984).
[20] K. Hahn and J. Kärger, J. Phys. Chem. B **102**, 5766 (1998).
[21] H. L. Tepper, J. P. Hoogenboom, N. F. A. van der Veget, and W. J. Briels, J. Chem. Phys. **110**, 11511 (1999).
[22] K. K. Mon and J. K. Percus, J. Chem. Phys. **117**, 2289 (2002).
[23] O. Flomenbom and A. Taloni, EPL **83**, 20004 (2008).
[24] L. Lizana and T. Ambjörnsson, Phys. Rev. Lett. **100**, 200601 (2008).
[25] C. Aslangul, J. Phys. A **33**, 851 (2000); Europhys. Lett. **44**, 284 (1998).
[26] K. Hahn *et al.*, Phys. Rev. Lett. **76**, 2762 (1996).
[27] T. Bandyopadhyay, EPL **81**, 16003 (2008).
[28] O. Flomenbom, Phys. Lett. A **374**, 4331 (2010).
[29] J. P. de Gennes, J. Chem. Phys. **55**, 572 (1971).
[30] J. Kärger and D. M. Ruthven, *Diffusion in Zeolites and Other Microscopic Solids* (Wiley, New York, 1992).
[31] G. Coupier, M. Saint Jean, and C. Guthmann, EPL **77**, 60001 (2007).
[32] P. H. Nelson and S. M. Auerbach, J. Chem. Phys. **110**, 9235 (1999).
[33] B. Lin, M. Meron, B. Cui, S. A. Rice, and H. Diamant, Phys. Rev. Lett. **94**, 216001 (2005).
[34] R. Shusterman, S. Alon, T. Gavrinyov, and O. Krichevsky, Phys. Rev. Lett. **92**, 048303 (2004).
[35] P. Demontis *et al.*, J. Chem. Phys. **120**, 9233 (2004); R. L. June *et al.*, *ibid.* **94**, 8232 (1990); U. Hong *et al.*, Zeolites **11**, 816 (1991).
[36] Q. H. Wei *et al.*, Science **287**, 625 (2000); C. Lutz *et al.*, Phys. Rev. Lett. **93**, 026001 (2004).
[37] P. M. Richards, Phys. Rev. B **16**, 1393 (1977).
[38] H. Bethe, Z. Phys. **71**, 205 (1931).
[39] D. R. Cox and D. V. Hinkley, *Theoretical Statistics* (Chapman and Hall, London/CRC, Boca Raton, 1979).
[40] E. Barkai and R. Silbey, Phys. Rev. Lett. **102**, 050602 (2009).
[41] O. Flomenbom, Phys. Lett. A **373**, 1405 (2009).
[42] See supplementary material at http://link.aps.org/supplemental/10.1103/PhysRevE.82.031126 for further discussion including including: A—Solutions for simple files. B—$P(\boldsymbol{x},t|\boldsymbol{x_0})$ for heterogeneous files. C—$P(r,t|r_0)$ for heterogeneous files. D—Calculations for $\tilde{D}_n$.